Synthesis, Physicochemical Properties, and Biological Evaluation of N-Substituted 2-Alkyl-3-hydroxy-4(1*H*)-pyridinones: Orally Active Iron Chelators with Clinical Potential

Paul S. Dobbin,† Robert C. Hider,*,† Adrian D. Hall,‡ Paul D. Taylor,§ Patience Sarpong,† John B. Porter,⊥ Gaoyi Xiao,∥ and Dick van der Helm∥

Department of Pharmacy, King's College London, Manresa Road, London, SW3 6LX, U.K., Department of Physics, The Royal Marsden Hospital, Downs Road, Sutton, Surrey, SM2 5PT, U.K., Department of Chemistry, University College London, Gower Street, London, WC1E 6BT, U.K., Department of Haematology, University College Hospital, London, WC1E 6HX, U.K., and Department of Chemistry, Oklahoma University, 620 Parrington Oval, Norman, Oklahoma 73019-0370

Received February 1, 1993

The synthesis of a range of novel bidentate ligands containing the chelating moiety 3-hydroxy-4(1*H*)-pyridinone is described. The pK_a values of the ligands and the stability constants of their iron(III) complexes have been determined. The crystal structures of one of the ligands and one of the iron(III) complexes are presented. The distribution coefficients of the ligands are reported and are related to the ability of the ligands to remove iron from hepatocytes. The influence of 3-hydroxy-4(1*H*)-pyridinones on oxidative damage to cells is described. In contrast to the iron chelator in current therapeutic use, desferrioxamine-B, many of the bidentate ligands described in this study are orally active in iron-overloaded mice.

There are a number of inherited disease states which are associated with the gradual accumulation of iron, β-thalassaemia major and thalassaemia intermedia being particularly well characterised.[1] Iron, due to its facile redox chemistry, is toxic when present in excess[2] and must be removed by chelation therapy. The naturally occurring siderophore desferrioxamine B was first demonstrated to increase excretion of iron in 1962,[3] and subsequent widespread use has demonstrated a definite prolonging of life in multiply transfused patients.[4] However, because the drug is inactive by mouth and has to be presented either subcutaneously or intravenously, compliance can be poor.[5]

During the worldwide search for an orally active specific iron chelator to replace desferrioxamine B, much effort has been channelled into the synthesis of catechol,[6] hydroxamate,[7] and carboxylate ligands.[8] This is a logical approach since the majority of natural siderophores (high affinity, low molecular weight, iron(III) multidentate ligands) are formed from one or more of these moieties.[9] Each of these chemical functions, however, has disadvantages when being considered for clinical use:[5] catechols are rapidly oxidized in the intestine, are generally poorly absorbed, and form charged iron(III) complexes;[10] hydroxamates are in principle susceptible to enzyme-catalyzed cleavage, and many possess poor oral bioavailability;[11] amino carboxylates are not sufficiently specific for iron(III)[5] and for oral presentation are best presented as ester pro-drugs.[12]

In view of these limitations, it was decided to investigate ligands, which although related in structure to both catechol and hydroxamate, might lack their relative instability under biological conditions. In particular, the ligands should be stable at strongly acid pH values and resistant to autoxidation and enzyme-catalyzed cleavage. The hydroxypyridinones 1-3 and the hydroxypyranones 4 (Figure 1) were considered as potential iron(III)-selective ligands, and preliminary investigation demonstrated their ability to chelate iron,[13] a finding confirmed by Scarrow *et al.*[14] The 3-hydroxy-4(1*H*)-pyridinones 1 and 3-hydroxy-2(1*H*)-pyridinones 2 have both been demonstrated to remove iron from iron-overloaded animals.[15,16] The 3-hydroxy-4(1*H*)-pyridinones 1 were found to be more effective than the other three molecular classes (2-4), and this is almost certainly directly related to their higher affinity for iron(III).[10,17]

In this paper we report the progress in the development of N-substituted 2-alkyl-3-hydroxy-4(1*H*)-pyridinones as orally active selective iron(III) chelators for clinical use. After description of synthetic pathways, we outline the investigation of physical and biochemical characteristics together with *in vitro* and *in vivo* iron removal studies. In conclusion, we compare the properties of an optimum hydroxypyridinone with those of desferrioxamine B.

Chemistry

All of the 1-substituted 2-alkyl-3-hydroxy-4(1*H*)-pyridinones in this study were synthesized utilizing the methodology of Harris and co-workers[18] (Scheme I). The commercially available 3-hydroxy-4(4*H*)-pyranones maltol and ethyl maltol[19] were benzylated in 90% aqueous methanol to give 5 and 6, respectively. Reaction of these adducts with primary amines was invariably performed by reflux in 50% aqueous ethanol with a catalytic amount of sodium hydroxide present. Where possible the benzylated pyridinones were isolated in a crystalline form as either the free base or the hydrochloride salt. Removal of the protecting benzyl group was achieved by catalytic hydrogenolysis to yield the bidentate chelators which were all isolated as the hydrochloride salts. The amide analogues 37 to 44 were obtained *via* reaction of the succinimidyl activated ester 18 with a variety of primary and secondary amines (Scheme II).

Determination of Solution Properties

3-Hydroxy-4(1*H*)-pyridinones 1 possess two pK_a values as indicated in Scheme III. These bidentate ligands also

† King's College London.
‡ The Royal Marsden Hospital.
§ University College London.
⊥ University College Hospital.
∥ Oklahoma University.

0022-2623/93/1836-2448$04.00/0

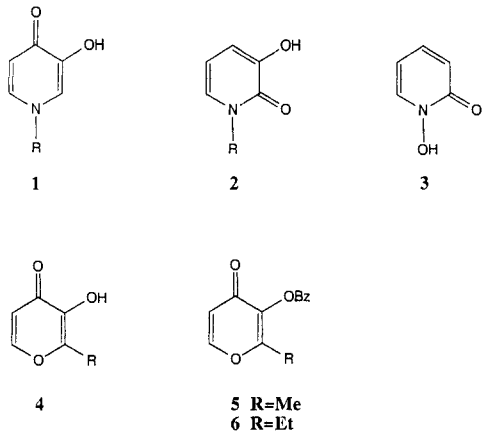

1 2 3

4 5 R=Me 6 R=Et

Figure 1. Structures of bidentate iron(III) ligands.

Scheme I

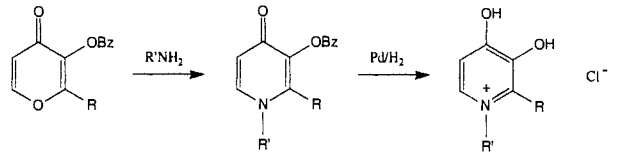

Scheme II

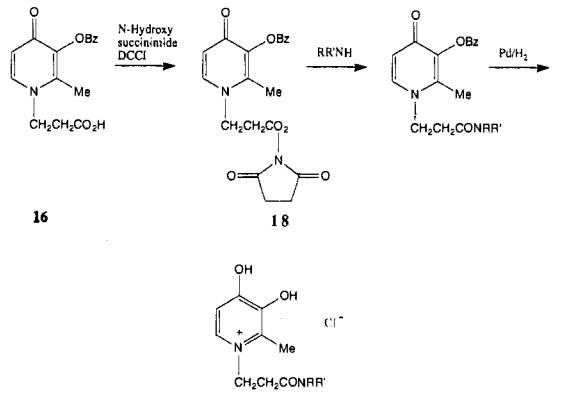

16 18

Scheme III

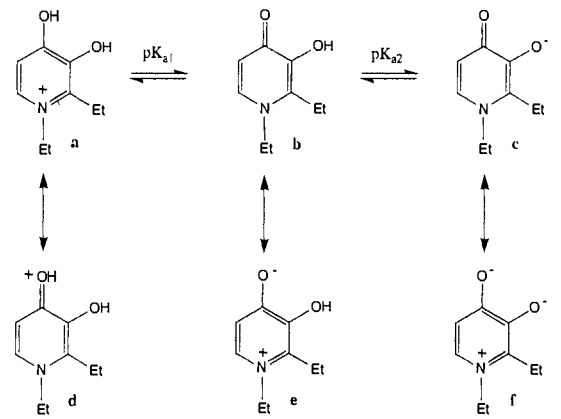

form a number of complexes with iron(III) so that aqueous solutions equilibrate to give mixtures in which the speciation depends on the metal ion, ligand, and hydrogen ion concentrations. A simple model of this system is shown in eq 1. This model has previously been shown to apply to 3-hydroxy-4(1*H*)-pyridinones.[17] Both the pK_a values and stability constants were obtained by global optimizations of parameters corresponding to titrations at several different ligand and iron(III) concentrations. The experimental conditions ensured that the most associated species predominated.

$$Fe^{3+} + L^- \rightleftharpoons FeL^{2+} \quad K_1 \qquad (1)$$

$$FeL^{2+} + L^- \rightleftharpoons FeL_2^{+} \quad K_2$$

$$FeL_2^{+} + L^- \rightleftharpoons FeL_3 \quad K_3$$

Distribution coefficients of the 3-hydroxy-4(1*H*)-pyridinones were determined in an aqueous/octanol system using a modified filter probe device.[20]

Biological Experiments

The rate of chelator-induced removal of iron from human serum transferrin and horse ferritin was monitored by spectrophotometric measurement. Chelator-induced efflux of iron across hepatocyte membranes was determined by quantification of ^{59}Fe. Iron-overloaded mice were used to establish the profile of ^{59}Fe excretion with time after administration of each chelator.

Results

Ligand pK_a Values. Some representative ligands have been studied by simultaneous spectrophotometric/potentiometric titrations. The optimized pK_a values obtained with the computer program NONLINGEN 15[21] are shown in Table I. The pK_{a1} values correspond to the protonation of the 4-oxo group and the pK_{a2} values to the dissociation of the 3-hydroxy group (Scheme III). The values were found to be relatively constant irrespective of the N-alkyl function.

Stability Constants of Iron(III) Complexes. For bidentate ligands the logarithm of the cumulative stability constants was determined. This value, log β_3, is obtained by summation of the logarithms of three stepwise equilibrium constants corresponding to eq 1. The optimized values are presented in Table II. Again, the values were found to be largely independent of the nature of the N-alkyl function.

Distribution Coefficients. Values of distribution coefficients between an aqueous phase buffered at pH 7.4 and octanol are presented in Tables IX and X. In general, the expected increase in distribution coefficient upon elongation of the alkyl chain was observed in the N-alkyl series (**20–28** and **48–53**), the N-alkylcarbamoyl series (**37–41** and **42–44**), and the hydroxyalkyl series (**32–34**). Surprisingly, the unsubstituted pyridinones **19** and **47** possess higher values than the corresponding *N*-methylpyridinones (**20** and **48**). The charged molecules (**35, 36, 45, 46**) possess low values. Some of the values presented in Tables IX and X are slightly different from those previously published.[16] The values presented in the previous study were produced by the "shake flask" method and are less accurate.

X-ray Crystallography. A stereoview of 1,2-diethyl-3-hydroxy-4(1*H*)-pyridinone hydrochloride (**49**·HCl) is shown in Figure 2. The bond distances of ligand **49** and its hydrochloride are listed in Table IV. The bond distances in **49** agree very well with those observed for its 2-methyl congener 1-ethyl-2-methyl-3-hydroxy-4-(1*H*)-pyridinone (**21**).[22,23] Like other 3-hydroxy-4(1*H*)-pyridinones[17,22–24] the heterocyclic ring of the neutral form is obviously in quinoid form **b** in Scheme III. On the other hand, the C(4)–O(2) bond is significantly longer (1.264 Å) than a pure ketone bond (1.210 Å). This provides the O(2) atom with a partial negative charge, resulting from resonance form **e** in Scheme III, which is important

Table I. Measurements Made at 22.5 °C, Ionic Strength 0.2

compd	R	R_1	pK_{a1}	pK_{a2}
57	H	H	3.34[a]	9.01[a]
19	Me	H	3.70	9.76
20	Me	Me	3.56	9.64
21	Me	Et	3.65	9.88
22	Me	nPr	3.62	9.92
24	Me	nBu	3.62	9.87

[a] Measurements by Scarrow *et al.*[14] at 25 °C, ionic strength 0.1.

Table II. Measurements Made at 22.5 °C, Ionic Strength 0.2

compd	R	R_1	$\log K_1$	$\log K_2$	$\log K_3$	$\log \beta_3$
57	H	H	14.2[a]	11.6[a]	9.3[a]	35.1
19	Me	H	15.4[b]	12.03	9.73	37.2
20	Me	Me	14.92	12.23	9.79	37.2
21	Me	Et	15.33	12.5[b]	9.90	37.7
22	Me	nPr	15.34	12.57	9.82	37.7
24	Me	nBu	15.34			

[a] Measurements by Scarrow *et al.*[14] at 25 °C, ionic strength 0.1. [b] Estimated values based on statistical and coulombic factors.

for chelation. This argument also explains why **49** forms relatively strong hydrogen bonding (O–H···O= C: 1.87 (3) Å) and crystallizes as centrosymmetric hydrogen bonded dimeric units, which is found in all other known 3-hydroxy-4-pyridinone crystal structures.[17,22-24]

In the crystal structure of **49**·HCl, the bond distances are comparable with those determined for 1,2-dimethyl-3-hydroxy-4(1*H*)-pyridinone hydrochloride (**20**).[17] Upon protonation of the carbonyl O(2) atom, there occurs a significant aromatic delocalization (form **a** in Scheme III) in which the C(4)–O(2) bond increases by 0.069 Å and the C(3)–C(4) and C(4)–(5) single bonds become shorter, while the C(2)–C(3) and C(5)–C(6) double bonds become longer. Meanwhile, the C(3)–O(1) bond shortens by 0.008 Å. The consistently shorter C(4)–O(2) bond against C(3)–O(1) bond, and longer C(3)–C(4) and C(4)–C(5) bonds against C(2)–C(3) and C(5)–C(6) bonds in the protonated ligands **49** and **20** suggest a contribution from resonance form **d** in Scheme III. There is a very strong hydrogen bond (1.68(3) Å) between the proton on the hydroxy O(1) atom and a water molecule.

An ORTEP plot of a single molecule for tris[1-(2′-methoxyethyl)-2-methyl-3-hydroxy-4-pyridinone]ferric trihydrate complex **58** (the tris complex of **29**) is depicted in Figure 3 with a numbering scheme, while its bond distances are listed in Table IV. When the bond distances in complex **58** are compared with its ligand,[25] there are several significant changes similar to those observed in the protonated ligand **49**. The C(3)–O(1) is reduced by 0.017 Å, while the C(4)–O(2) is greatly increased by 0.042 Å in complex **58** upon metal chelation. The delocalization in the C–O bonds results in obvious averaging of the single and double C–C bonds in the ring. Therefore, the resonance form similar to **f** in Scheme III is important. All the above geometric changes upon chelation have been found in complexes of tris(3-hydroxy-4(1*H*)-pyridinones) with metal(III) cations.[22,23,26-28]

Ability of 3-Hydroxy-4(1*H*)-pyridinones To Remove Iron from Iron-Proteins. Transferrin. The addition of the colorless chelator solutions (100 μM) to Fe(III)–transferrin (50 μM) resulted in the removal of some iron from the protein as indicated by the change in absorbance in the visible wavelength region. The kinetics of removal were found to be biphasic, and after 2 h approximately 50% of the iron was removed. There was no significant difference in the behavior of any of the chelators investigated (Table V) irrespective of the nature of the N-substituent. Desferrioxamine B was essentially inactive in this assay.

Table III.

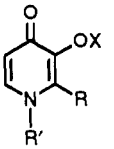

compd	R	R′	X
7	Me	H	Bz
8	Et	H	Bz
9	Me	Me	Bz
10	Me	Et	Bz
11	Me	CH_2CH_2OMe	Bz
12	Me	CH_2CH_2OH	Bz
13	Me	$CH_2CH_2CH_2OH$	Bz
14	Et	Me	Bz
15	Et	CH_2CH_2OH	Bz
16	Me	$CH_2CH_2CO_2H$	Bz
17	Me	$CH_2CH_2CH_2CO_2H$	Bz
19	Me	H	H
20	Me	Me	H
21	Me	Et	H
22	Me	nPr	H
23	Me	iPr	H
24	Me	nBu	H
25	Me	nPent	H
26	Me	nHex	H
27	Me	nOct	H
28	Me	nDec	H
29	Me	CH_2CH_2OMe	H
30	Me	CH_2-CH_2-CH_2OEt	H
31	Me	$CH(CH_3)CH_2OMe$	H
32	Me	CH_2CH_2OH	H
33	Me	$CH_2CH_2CH_2OH$	H
34	Me	$CH_2CH_2CH_2CH_2OH$	H
35	Me	$CH_2CH_2CO_2H$	H
36	Me	$CH_2CH_2CH_2CO_2H$	H
37	Me	$CH_2CH_2CONHMe$	H
38	Me	$CH_2CH_2CONHEt$	H
39	Me	$CH_2CH_2CONHnPr$	H
40	Me	$CH_2CH_2CONHisoPr$	H
41	Me	$CH_2CH_2CONHnBut$	H
42	Me	$CH_2CH_2CONMe_2$	H
43	Me	$CH_2CH_2CONMeEt$	H
44	Me	$CH_2CH_2CONEt_2$	H
45	Me	$CH_2CH_2NH_3^+Cl^-$	H
46	Me	$CH_2CH_2CH_2NH_3^+Cl^-$	H
47	Et	H	H
48	Et	Me	H
49	Et	Et	H
50	Et	nPr	H
51	Et	iPr	H
52	Et	nBu	H
53	Et	nHex	H
54	Et	CH_2CH_2OMe	H
55	Et	$CH_2CH_2CH_2OEt$	H
56	Et	CH_2CH_2OH	H
57	H	H	H

Ferritin. Incubation of ferritin (containing iron cores with an equivalent concentration of 450 μM) with colorless chelator solutions (5 mM) resulted in the slow removal of iron, as monitored by the increase in absorbance at 450 nm of the filtrate after ultrafiltration of the incubate. The kinetics of iron removal were monophasic, and after 24 h approximately 25% of the iron core was mobilized (Table V). There was no significant difference in rate of removal of iron by the neutral ligands, although both the charged molecules **36** and **45** were found to be less efficient at iron removal. Desferrioxamine B was much less efficient than the neutral pyridinones. These results are in broad agreement with those previously reported.[29]

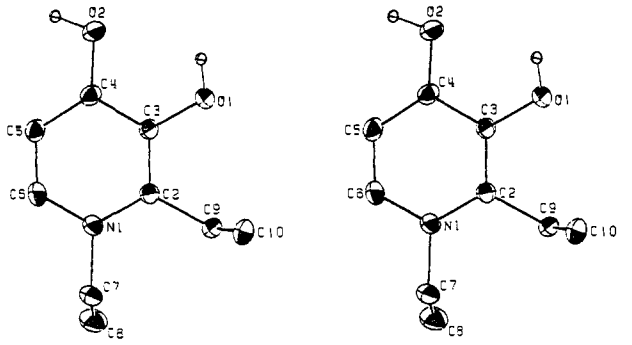

Figure 2. Stereoview of molecule **49**·HCl showing numbering scheme. The H_2O and Cl^- are omitted for the purpose of numbering.

Table IV. Bond Distances (Å) for **49**·HCl, **49**, and **58** with esd's in Parentheses

	49	49·HCl	58
Fe–O(1)			2.001(2)
Fe–O(2)			2.047(3)
N(1)–C(2)	1.368(2)	1.379(2)	1.382(4)
N(1)–C(6)	1.354(2)	1.349(2)	1.353(7)
N(1)–C(7)	1.488(2)	1.480(2)	1.495(5)
C(2)–C(3)	1.388(2)	1.375(2)	1.399(5)
C(2)–C(9)	1.502(2)	1.509(2)	
C(2)–C(11)			1.489(7)
C(3)–C(4)	1.406(2)	1.433(2)	1.411(7)
C(3)–O(1)	1.346(2)	1.354(2)	1.337(5)
C(4)–C(5)	1.392(2)	1.421(2)	1.410(5)
C(4)–O(2)	1.333(2)	1.264(2)	1.306(4)
C(5)–C(6)	1.368(2)	1.361(2)	1.359(5)
C(7)–C(8)	1.513(2)	1.510(3)	1.498(7)
C(8)–O(9)			1.363(9)
O(9)–C(10)			1.575(4)
C(9)–C(10)	1.534(2)	1.525(5)	

Ability of 3-Hydroxy-4(1*H*)-pyridinones To Remove Iron from Hepatocytes. Rat hepatocytes were cultured overnight, preincubated with ^{59}Fe–transferrin, and then incubated with a range of chelators.[30] The rate of efflux of ^{59}Fe from the hepatocytes was monitored in the presence and absence of chelator, and the data are presented as the percentage of the ^{59}Fe efflux occurring in the absence of the chelator. Figure 4 shows the effect of increasing chelator concentration on ^{59}Fe release from hepatocytes, and Figure 5 shows the effect of the same chelators on LDH leakage from intact cells and on lipid peroxidation as estimated by measurement of cellular MDA at the end of 6 h of incubation. It can be seen that **29**, which is relatively lipophilic compared with **20**, is more effective at mobilizing intracellular iron at all concentrations studied (Figure 4) without producing significant cell damage. Indeed, there is a small decrease in LDH leakage at 100 μM with both **20** and **29** compared with control cells suggesting that low concentrations of these compounds may be beneficial to hepatocytes in culture. With increasing chelator concentrations, MDA content of the cells falls progressively with a more pronounced effect in the relatively hydrophilic **20** compared with the relatively lipophilic **29** (Figure 5).

There is a clear correlation between distribution coefficient *D* of a range of pyridinones and their efficiency of iron removal (Figure 6). Compounds with *D* values less than 0.5 are not particularly efficient at mobilizing iron, and there is an onset of a plateau effect at values greater than 1.5. Thus, a *D* value close to unity appears to be optimal for the pyridinone-facilitated removal of iron from hepatocytes. 1-(2′-Methoxyethyl)-2-methyl-3-hydroxy-4(1*H*)-pyridinone (**29**) is the single exception from this relationship, where with $D = 0.39$ it causes efficient mobilization of iron. With all pyridinones possessing *D* values < 2.0 there is no detectable cell damage as monitored by LDH release (see, for instance, Figure 5). The critical nature of both the affinity constant (log β_3) and *D* on the iron mobilization process is demonstrated in a comparative study of different iron ligand classes (Table VI). The closely related 2-pyridine aldoxime and 3-hydroxy-2(1*H*)-pyridinone (**2**), each of which are neutral at pH 7.4, fail to mobilize iron. This undoubtedly relates to their lower affinity constants for iron(III). 8-Hydroxyquinoline, which does possess a sufficiently high affinity constant, also possesses a high *D* value (80.0) and consequently is toxic to the cells as is demonstrated by the release of LDH (Table VI).

Mobilization of Iron from Iron-Overloaded Mice. Iron-overloaded mice[31] were treated either orally or intraperitoneally with buffered chelator solutions, and the chelator-induced excretion (urine and feces) of ^{59}Fe was monitored. Dose responses for the oral administration of the pyridinones **20**, **29**, and **49** are presented in Figure 7a. All three compounds are remarkably active, the most hydrophilic (**20**) being the least efficient scavenger. In contrast to desferrioxamine B, which is not orally active, the 3-hydroxy-4(1*H*)-pyridinones are effective when administered either intraperitoneally or orally (Figure 7b). Indeed, pyridinone **29** is far more active than desferrioxamine when presented intraperitoneally.

Discussion

Iron(III) Binding Properties. The affinity measurements in this study demonstrate the high affinity of 3-hydroxy-4(1*H*)-pyridinones for iron(III); the log β_3 value for 1,2-dimethyl-3-hydroxy-4(1*H*)-pyridinone (**20**), for instance, was determined in this study as 36.9, which compares favorably with the value 35.9 independently determined by Motekaitis and Martell.[32] (The small difference between these two values could partially result from the different temperatures used, namely 22.5 and 25 °C.) This value is higher than those associated with closely related dioxo-bidentate ligands (Table VII). Indeed, although the 4-pyridinones appear to be weaker ligands for iron(III) than catechol, catechol has a much greater affinity for protons, and consequently in the pH range 2–8 the 4-pyridinone will compete more effectively for iron(III) than catechol. This difference is highlighted by the different pM values of the two ligands, catechol, 15.1, and 4-pyridinone, 20.0.[33] Thus, the 3-hydroxy-4(1*H*)-pyridinone moiety appears to be the optimal dioxo-bidentate ligand for iron(III) at physiological pH values. The partial negative charge on the carbonyl oxygen atom in the deprotonated ligand ion (Scheme III, **f**), leads to more than one negative charge over the two oxygen atoms bonded to the iron atom. This is the reason for the large complexation constants of the 4-pyridinones when compared with the other closely related ligands (Table VII). The delocalization of charge on the 4-carbonyl function also gives rise to its acidic character ($pK_{a1} = 3.6$). The extensive delocalization of charge in this molecular class is unambiguously demonstrated by the X-ray studies (Table IV). Although there are three complex types, ML, ML_2 and ML_3 (eq 1), the 1:3 complex (Figure 3) predominates at neutral pH values due to the extreme avidity of the 4-pyridinone ligand for iron(III). This property is clearly demonstrated in the speciation plot for 1-ethyl-

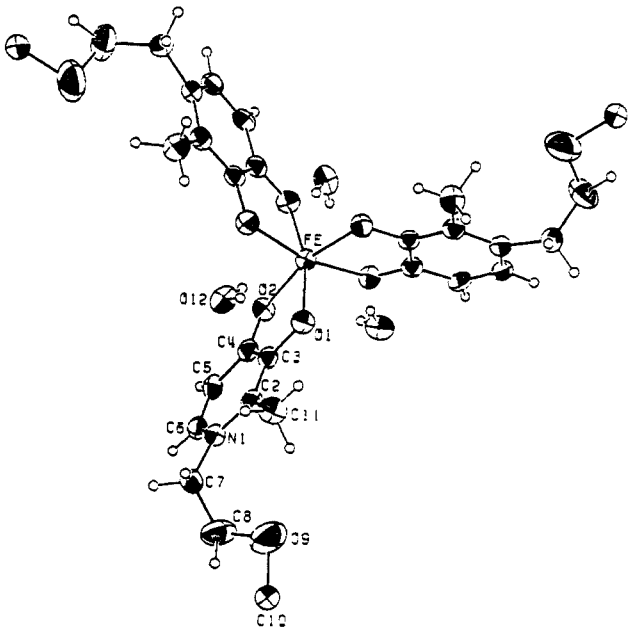

Figure 3. ORTEP plot of a single molecule of the iron(III) complex of pyridinone **29**.

Table V. Percentage of Removal of Iron from Transferrin and Ferritin

ligand	% iron removed[a] transferrin	ferritin
20	54 ± 2	34 ± 2.5
22	52 ± 3	28 ± 1.1
23	51 ± 3	26 ± 1.2
24	52 ± 4	
29	55 ± 2	28 ± 2.0
30	49 ± 3	
32	47 ± 4	29 ± 0.8
36	53 ± 6	12 ± 1.1
45	56 ± 3	23 ± 4.1
desferrioxamine	5 ± 2	11 ± 2.2
control	0	0

[a] Mean of 3 ± SE.

2-methyl-3-hydroxy-4(1*H*)-pyridinone (**21**) (Figure 8). Thus, the major form of complexed iron under biological conditions is hexacoordinated (Figure 3), and as such is unlikely to generate oxygen radicals under aerobic conditions.[5]

A further important observation to emerge from these studies is that a range of different N-substitutions failed to influence dramatically the affinity for protons (Table I) or for iron(III) (Table II). This observation is indirectly confirmed by X-ray studies where the bond lengths of the coordinating oxygen atoms and the distances of those oxygen atoms to the iron atom remained relatively constant among a range of pyridinones with varying N-substituents (58 present results).[23,27] Thus, it has been possible to design a wide range of 4-pyridinones with different biodistribution properties while retaining a constant affinity for iron(III).

Competition Studies with Iron-Transport and Storage Proteins. Iron is transported in mammalian blood on the glycoprotein transferrin; thus, iron is transferred bound to this protein from the intestine and the liver to tissues that require a regular supply of iron, for instance, the bone marrow. The high affinity of transferrin for iron ensures that the concentration of other forms of iron in the plasma are vanishingly small, thereby exerting a powerful antibacterial and antifungal influence.[36] The possibility of exchange of iron between transferrin and

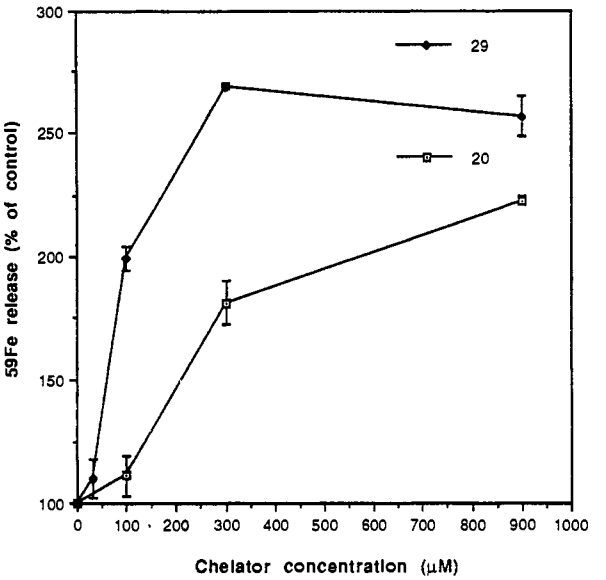

Figure 4. Hepatocyte ^{59}Fe release by hydroxypyridinone chelators (**20** and **29**). Hepatocytes derived from rat liver were placed on collagen plates and pulsed with [^{59}Fe]transferrin. Hepatocytes were subsequently exposed for 6 h to the chelators at the indicated concentrations. The mean of six independent determinations is shown with the standard error.

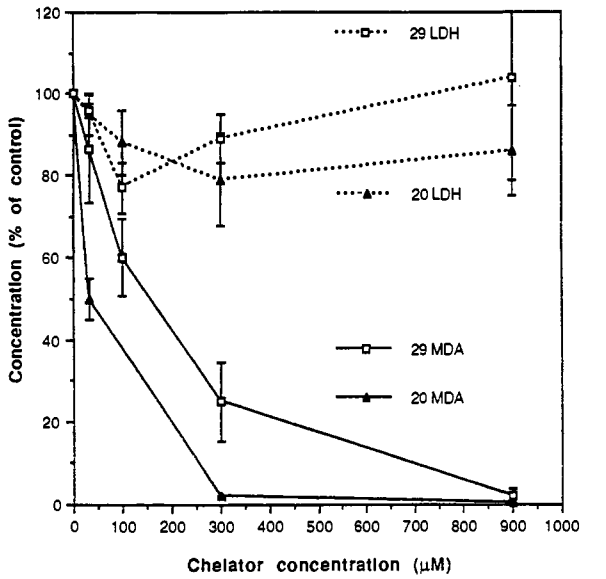

Figure 5. Influence of hydroxypyridinone chelators (**20** and **29**) on the release of lactate dehydrogenase (LDH) from hepatocytes and the production of malonyl dialdehyde by hepatocytes. Rat hepatocytes were incubated for 6 h on collagen plates. The mean of six independent determinations is shown with the standard error.

high affinity chelators is therefore a matter of considerable importance. To be clinically useful it is probably ideal that iron-scavenging molecules should not take iron from transferrin in view of the central role this molecule plays in iron metabolism. Most of the dioxo-bidentate ligands do not possess a sufficiently high affinity for iron(III) to compete with apotransferrin; however, the 3-hydroxy-4(1*H*)-pyridinone class, by virtue of their high p*M* value,[33] compete with transferrin at relatively high concentrations (10^{-3} M) (Table V). However, at lower concentrations of 10^{-4}–10^{-6} M, namely those likely to be experienced clinically, 4-pyridinoneiron(III) complexes donate iron to apotransferrin.[37]

The major intracellular storage form of iron is ferritin.

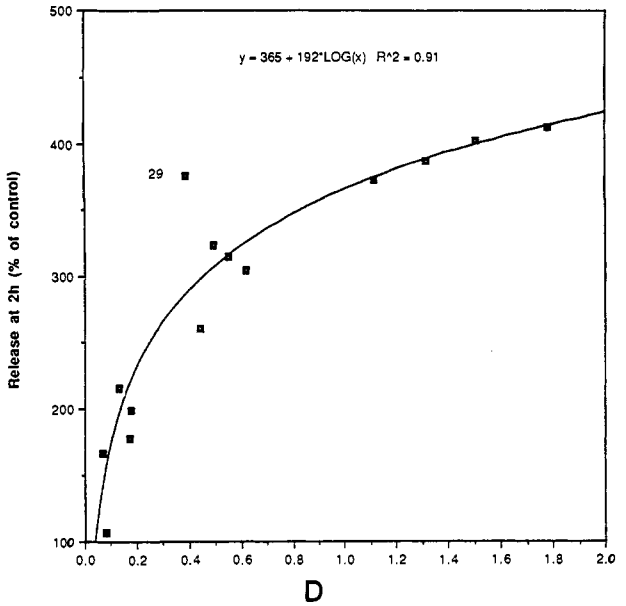

Figure 6. Relationship between distribution coefficients (D) and ability of hydroxypyridinones to remove iron from rat hepatocytes. Incubation conditions were as indicated in Figure 3.

Table VI. Percentage of Mobilization of Iron and Percentage of Release of Lactic Dehydrogenase (LDH) from Rat Hepatocytes

ligand	% mobilization of iron (2 h)	% LDH release	log β_3 (Fe III)
(22)	252 ± 14	105 ± 20	37
8-hydroxyquinoline	110 ± 8	260 ± 56	37
2-pyridine aldoxime	108 ± 6	108 ± 18	30
1-ethyl-3-hydroxy-2(1*H*)-pyridinone (2, (R = Et))	115 ± 9	102 ± 15	32

Ferritin consists of a protein shell surrounding an aqueous cavity in which water may be replaced by an "iron core" of the mineral ferrihydrite containing up to 4500 iron atoms.[38] In accumulating or removing iron from the core, access to the cavity is achieved *via* aqueous channels which penetrate the protein shell. Once stored in the core, the iron atoms are less liable to enter autoxidation reactions, which lead to the generation of potentially toxic oxygen radicals. Hexadentate ligands such as desferrioxamine B are too large to enter the pores of the ferritin molecule and consequently are relatively inefficient at removing iron from ferritin (Table V). In contrast, the 3-hydroxy-4(1*H*)-pyridinones are capable of removing iron from ferritin, albeit at a rather slow flux. Surprisingly, the bulk and hydrophobicity of the N-substituent has little effect on the efficiency of iron removal from ferritin, although negatively charged ligands are less effective (Table V). The rate-determining step for the removal of iron appears to be solubilization from the iron core.[29]

Iron Removal from Hepatocytes and Mice. The wide range of distribution coefficients obtained for the 3-hydroxy-4(1*H*)-pyridinones utilized in this study (0.001–750) has facilitated a systematic analysis of the relationship between membrane permeability and the efficiency of iron removal from intact cells and whole animals. The pK_a values of the 4-pyridinones are similar, falling in the ranges 3.3–3.7 and 9.0–9.9; thus, the predominant species in solution over the pH range 5–8 bears net zero charge (Scheme III, **b** and **e**).

Thus with molecular weights falling in the range 125–220, good membrane permeation is predicted for molecules with distribution coefficients >0.1. Indeed, ligands with distribution coefficients >0.5 were found to mobilize iron from hepatocytes extremely efficiently (Figure 6). 4-Pyridinones with distribution coefficients >5.0 were found to be toxic to cells.[16,39] Thus, although the N-substituent has little influence on the affinity of the 4-pyridinone for iron(III), it exerts a major effect on the ability of chelators

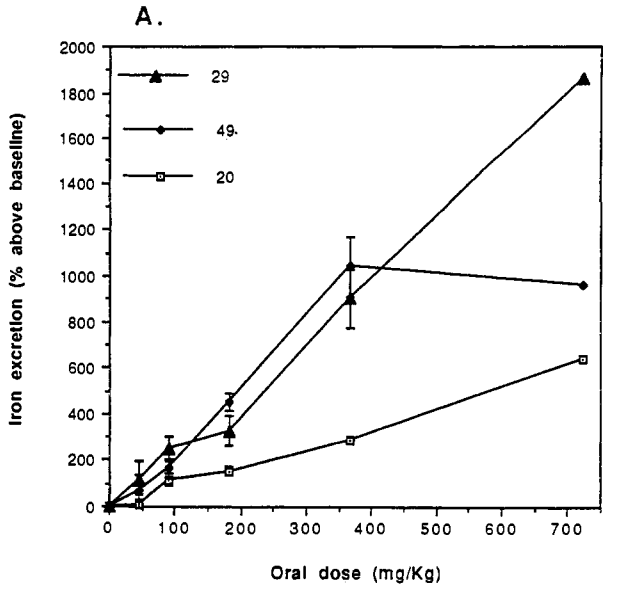

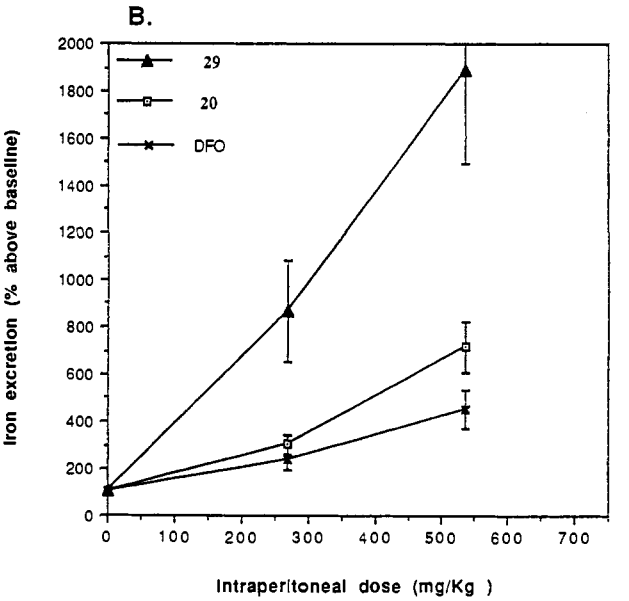

Figure 7. Removal of ^{59}Fe from iron-overloaded mice by chelators at various doses: (A) oral dosing, (B) intraperitoneal dosing. Mice were loaded with iron dextran, labeled with [^{59}Fe]lactoferrin, and allowed to stabilize for 3 weeks. After base-line excretion rates were recorded, chelators were administered. The amount of ^{59}Fe in the urine and feces over the next 24 h was measured with a γ-counter. The mean of four independent determinations is shown with the standard error.

Table VII. pK_a and log β_3 Values for Bidentate Ligands

	pK_{a2}	pK_{a1}	log β_3
catechol[a]	13.3	9.2	44.9
3-hydroxy-4(1*H*)-pyridinone (1)	9.6	3.6	36.9
3-hydroxy-2(1*H*)-pyridinone[b] (2)	8.8		32.3
1-hydroxy-2(1*H*)-pyridinone[c] (3)	5.8		26.9
3-hydroxy-4(4*H*)-pyranone[d] (4, R = Me)	8.7		28.4
acetohydroxamic acid[a]	9.4		28.3

[a] Reference 34. [b] Reference 15. [c] Reference 14. [d] Reference 35.

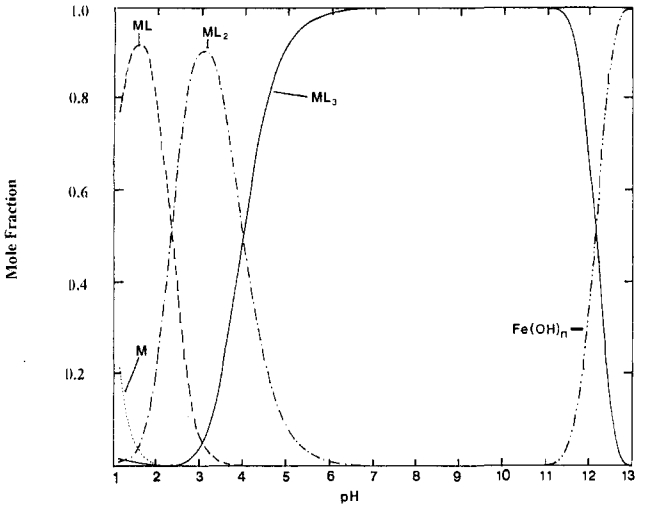

Figure 8. Speciation plot of 1-ethyl-2-methyl-3-hydroxy-4(1*H*)-pyridinone (**21**) and iron(III). Concentration of **21**, 4×10^{-4} M, concentration of iron(III), 1×10^{-4} M. The following parameters were incorporated into the model for this system: log K_{11} ML = 15.3; log K_{12} ML_2 = 12.5; log K_{13} ML_3 = 9.9; pK_{a1} = 3.62; pK_{a2} = 9.88. ML_1 ML_2 and ML_3 are the 1:1, 1:2, and 1:3 iron/**21** complexes, respectively.

to scavenge iron from intact cells and their associated toxicity. The reason for the anomalous behavior of **29** (Figure 6) is not clear; nevertheless, the potent activity observed in the hepatocyte system is mirrored in studies with iron-overloaded mice. In this work **29** was one of the most potent 4-pyridinones studied (Figure 7).

In contrast to desferrioxamine B, the 3-hydroxy-4(1*H*)-pyridinones are orally active. Compounds with distribution coefficients in the range 0.5–2.0 are more effective than those with lower values (<0.2).[40] More extensive biological studies are in progress with this promising family of molecules. Formal toxicity studies have been undertaken with **49** and this molecule, together with **20**, is currently the subject of clinical trials.[41-43]

Experimental Section

General Procedures. Melting points are uncorrected. IR spectra were recorded on a Perkin-Elmer 298. Proton NMR spectra were determined with a Perkin-Elmer R32 (90 MHz). Mass spectra were taken using a Vacuum Generators 16F (35 eV). Elemental analyses were performed by Butterworth Laboratories Limited, Teddington, Middlesex. Full spectroscopic and analytical data are available as supplementary material.

2-Ethyl-3-(benzyloxy)-4(4*H*)-pyranone (6). To a solution of ethyl maltol (196 g, 1.4 mol) in methanol (1800 mL) was added sodium hydroxide (60 g, 1.5 mol) dissolved in water (200 mL) followed by benzyl chloride (190 g, 1.50 mol) and the mixture refluxed for 6 h. After removal of solvent by rotary evaporation the resultant oil was taken up in dichloromethane (750 mL) and washed with 5% aqueous sodium hydroxide (2 × 750 mL) followed by water (2 × 750 mL). The organic fraction was then dried over anhydrous sodium sulfate, filtered, and rotary evaporated to yield an orange oil which solidified on cooling, recrystallization from diethyl ether giving colorless needles (255 g, 79%): mp 33–34 °C. Anal. ($C_{14}H_{14}O_3$) C, H.

An analogous procedure using maltol gave 2-methyl-3-(benzyloxy)-4(4*H*)-pyranone (**5**) (83%): mp 53–55 °C (lit.[18a] oil). Anal. ($C_{13}H_{12}O_3$) C, H.

2-Ethyl-3-(benzyloxy)-4-hydroxypyridine (8). To a solution of **6** (28 g, 0.12 mol) in ethanol (200 mL) was added 35% aqueous ammonia (400 mL) and the mixture refluxed for 18 h. Removal of solvent by rotary evaporation gave an oil which solidified on addition of acetone and cooling, recrystallization from ethanol yielding colorless prisms (24 g, 89%): mp 168–169 °C. Anal. ($C_{14}H_{15}NO_2$) C, H, N.

An analogous procedure using **5** gave 2-methyl-3-(benzyloxy)-4-hydroxypyridine (**7**) (88%): mp 165–166 °C (lit.[18a] mp 162–163 °C). Anal. ($C_{13}H_{13}NO_2$) C, H, N.

2-Methyl-3,4-dihydroxypyridine Hydrochloride (19). A solution of **7** (20 g, 0.093 mol) in ethanol (270 mL)/water (30 mL) was adjusted to pH 1 with hydrochloric acid prior to hydrogenolysis for 4 h in the presence of 5% Pd/C catalyst (1 g). Filtration followed by rotary evaporation gave a white solid, recrystallization from ethanol/diethyl ether yielding a white powder (15.1 g, 95%): mp 172–173 °C. Anal. ($C_6H_8NO_2Cl \cdot {}^1/_2H_2O$) C, H, N.

An analogous procedure using **8** gave 2-ethyl-3,4-dihydroxypyridine hydrochloride **47** (90%): mp 166–167 °C. Anal. ($C_7H_{10}ClNO_2$) C, H, N.

1,2-Dimethyl-3-(benzyloxy)-4(1*H*)-pyridinone Hydrochloride (9). To a solution of **5** (25 g, 0.12 mol) in ethanol (200 mL)/water (200 mL) was added 40% aqueous methylamine (14 g, 0.18 mol) followed by 2 N sodium hydroxide solution (10 mL) and the mixture refluxed for 18 h. After adjustment to pH 1 with hydrochloric acid, the volume was reduced to 200 mL by rotary evaporation prior to addition of water (200 mL) and washing with diethyl ether (400 mL). Subsequent adjustment of the aqueous fraction to pH 7 with 10 N sodium hydroxide solution was followed by extraction into dichloromethane (3 × 400 mL), the organic layers then being dried over anhydrous sodium sulfate, filtered, and rotary evaporated to give an orange oil. This oil was dissolved in ethanol/hydrochloric acid and rotary evaporated, the resulting white solid being recrystallized from ethanol/diethyl ether to give a white powder (26 g, 85%): mp 207–208 °C. Anal. ($C_{14}H_{16}ClNO_2$) C, H, N.

Analogous reaction of **5** with ethylamine, 2-methoxyethylamine, ethanolamine, or 3-hydroxypropylamine and of **6** with methylamine or ethanolamine gave compounds **10–15** as shown in Table VIII.

1,2-Dimethyl-3-hydroxy-4(1*H*)-pyridinone Hydrochloride (20). A solution of **9** (20 g, 0.075 mol) in ethanol (270 mL)/water (30 mL) was subjected to hydrogenolysis for 4 h in the presence of 5% Pd/C catalyst (1 g). Filtration followed by rotary evaporation gave a white solid, recrystallization from ethanol/diethyl ether yielding a white powder (13 g, 89%): mp 189–190 °C. Anal. ($C_7H_{10}ClNO_2 \cdot H_2O$) C, H, N.

Analogous reaction of **10–15** gave compounds **21**, **29**, **32**, **33**, **48**, and **56**, respectively, as shown in Table IX.

1-Propyl-2-methyl-3-hydroxy-4(1*H*)-pyridinone Hydrochloride (22). To a solution of **5** (25 g, 0.12 mol) in ethanol (200 mL)/water (200 mL) was added propylamine (10.6 g, 0.18 mol) followed by 2 N sodium hydroxide solution (10 mL) and the mixture refluxed for 18 h. After an extraction procedure identical to that used in the preparation of **9** an orange oil was obtained, which was subsequently dissolved in ethanol (270 mL)/water (30 mL) and adjusted to pH 1 with hydrochloric acid prior to hydrogenolysis for 4 h in the presence of 5% Pd/C catalyst (1 g). Filtration followed by rotary evaporation gave a white solid, recrystallization from ethanol/diethyl ether yielding a white powder (19 g, 81%): mp 206–207 °C. Anal. ($C_9H_{14}ClNO_2$) C, H, N.

Analogous syntheses starting with reaction of **5** or **6** with ethylamine, propylamine, isopropylamine, butylamine, pentylamine, hexylamine, octylamine, 2-methoxyethylamine, 3-ethoxypropylamine, (±)-2-amino-1-methoxypropane, 3-hydroxypropylamine, and 4-hydroxybutylamine gave compounds **21–27**, **29–31**, **33**, **34**, and **49–55** as shown in Table IX.

1-(2′-Carboxyethyl)-2-methyl-3-(benzyloxy)-4(1*H*)-pyridinone (16). To a solution of **5** (25 g, 0.12 mol) in ethanol (300 mL) was added β-alanine (12.5 g, 0.14 mol) dissolved in water (300 mL) followed by 10 N sodium hydroxide solution until pH 13 was attained. After reflux for 18 h, the resulting solution was reduced in volume to 200 mL by rotary evaporation prior to adjustment to pH 4 with hydrochloric acid and extraction into dichloromethane (3 × 250 mL). The organic fractions were then dried over anhydrous sodium sulfate, filtered, and rotary evaporated to give an orange oil which solidified on addition of acetone and cooling, recrystallization from ethanol/diethyl ether giving a yellow powder (24 g, 72%): mp 170–171 °C. Anal. ($C_{16}H_{17}NO_4$) C, H, N.

Table VIII. Syntheses of 1-Substituted 2-Alkyl-3-(benzyloxy)-4(1*H*)-pyridinone Hydrochlorides

compd	R	R[1]	mp, °C	% yield	formula	anal.
9	Me	Me	207–208	85	$C_{14}H_{16}NO_2Cl$	C,H,N
10	Me	Et	178–179	85	$C_{15}H_{16}NO_2Cl$	C,H,N
11	Me	$CH_2CH_2OCH_3$	150–151	81	$C_{16}H_{20}NO_3Cl \cdot H_2O$	C,H,N
12	Me	CH_2CH_2OH	205–206	73	$C_{15}H_{16}NO_3Cl$	C,H,N
13	Me	$CH_2CH_2CH_2OH$	160–161	77	$C_{16}H_{20}NO_3Cl$	C,H,N
14	Et	Me	176–177	80	$C_{15}H_{16}NO_2Cl$	C,H,N
15	Et	CH_2CH_2OH	169–170	82	$C_{16}H_{20}NO_3Cl$	C,H,N

Table IX. Synthesis of 1-Substituted 2-Alkyl-3-hydroxy-4(1*H*)-pyridinone Hydrochlorides and Their Distribution Coefficients between an Aqueous Phase Buffered at pH 7.4 and Octanol

R	R	R[1]	mp, °C	% yield (from 5 or 6)	formula	anal.	distribn coeff
19	Me	H	172–173	84	$C_6H_8NO_2Cl \cdot {}^1/_2H_2O$	C,H,N	0.32 ± 0.01 (n = 10)
20	Me	Me	189–190	76	$C_7H_{10}NO_2Cl \cdot H_2O$	C,H,N	0.17 ± 0.01 (n = 10)
21	Me	Et	205–206	74	$C_8H_{12}NO_2Cl$	C,H,N	0.49 ± 0.01 (n = 25)
22	Me	Pr	206–207	81	$C_9H_{14}NO_2Cl$	C,H,N	1.51 ± 0.01 (n = 25)
23	Me	iPr	225–226	72	$C_9H_{14}NO_2Cl$	C,H,N	1.12 ± 0.01 (n = 5)
24	Me	Bu	199–200	73	$C_{10}H_{16}NO_2Cl$	C,H,N	5.05 ± 0.02 (n = 11)
25	Me	pentyl	165–166	68	$C_{11}H_{16}NO_2Cl$	C,H,N	17.4 ± 0.2 (n = 24)
26	Me	hexyl	166–167	70	$C_{12}H_{20}NO_2Cl$	C,H,N	79 ± 5 (n = 6)
27	Me	octyl	134–135	59	$C_{14}H_{24}NO_2Cl$	C,H,N	750 ± 100 (n = 12)
28	Me	decyl	140–141	57	$C_{16}H_{28}NO_2Cl$	C,H,N	insoluble
29	Me	$CH_2CH_2OCH_3$	173–174	72	$C_9H_{14}NO_3Cl$	C,H,N	0.39 ± 0.01 (n = 5)
30	Me	$(CH_2)_3OCH_2CH_3$	145–146	76	$C_{11}H_{16}NO_3Cl$	C,H,N	1.32 ± 0.01 (n = 5)
31	Me	$CH(CH_3)CH_2OCH_3$	117–118	55	$C_{10}H_{16}NO_3Cl \cdot H_2O$	C,H,N	0.55 ± 0.09 (n = 5)
32	Me	CH_2CH_2OH	156–157	62	$C_8H_{12}NO_3Cl \cdot H_2O$	C,H,N	0.08 (n = 3)
33	Me	$CH_2CH_2CH_2OH$	120–121	67	$C_9H_{14}NO_3Cl$	C,H,N	0.132 ± 0.001 (n = 4)
34	Me	$(CH_2)_4OH$	144–145	60	$C_{10}H_{16}NO_3Cl$	C,H,N	0.181 ± 0.001 (n = 5)
35	Me	$CH_2CH_2CO_2H$	207–208	67	$C_9H_{12}NO_4Cl$	C,H,N	<0.001
36	Me	$(CH_2)_3CO_2H$	225–226	63	$C_{10}H_{14}NO_4Cl$	C,H,N	<0.001
45	Me	$CH_2CH_2NH_3Cl$	284–285	61	$C_8H_{14}N_2O_2Cl_2$	C,H,N	0.028 ± 0.001 (n = 4)
46	Me	$CH_2CH_2CH_2NH_3Cl$	260–261	68	$C_8H_{16}N_2O_2Cl_2 \cdot H_2O$	C,H,N[a]	0.008 ± 0.003 (n = 5)
47	Et	H	166–167	80	$C_7H_{10}NO_2Cl$	C,H,N	1.11 ± 0.03 (n = 8)
48	Et	Me	219–220	73	$C_8H_{12}NO_2Cl$	C,H,N	0.624 ± 0.003 (n = 5)
49	Et	Et	188–189	75	$C_9H_{14}NO_2Cl$	C,H,N	1.78 ± 0.01 (n = 5)
50	Et	Pr	143–144	75	$C_{10}H_{16}NO_2Cl \cdot H_2O$	C,H,N	5.04 ± 0.02 (n = 5)
51	Et	iPr	206–207	53	$C_{10}H_{16}NO_2Cl$	C,H,N	5.4 ± 1.0 (n = 7)
52	Et	Bu	155–156	60	$C_{11}H_{16}NO_2Cl$	C,H,N	16.6 ± 0.8 (n = 10)
53	Et	hexyl	104–105	55	$C_{13}H_{22}NO_2Cl$	C,H,N	189 ± 5 (n = 5)
54	Et	$CH_2CH_2OCH_3$	132–133	58	$C_{10}H_{16}NO_3Cl$	C,H,N	1.1 ± 0.2 (n = 5)
55	Et	$(CH_2)_3OCH_2CH_3$	100–101	58	$C_{12}H_{20}NO_3Cl$	C,H,N	5.2 ± 0.2 (n = 5)
56	Et	CH_2CH_2OH	153–154	71	$C_9H_{14}NO_3Cl$	C,H,N	0.22 ± 0.01 (n = 5)

[a] N: calcd 10.26; found 9.76.

An analogous procedure using 4-aminobutyric acid gave 1-(3′-carboxypropyl)-2-methyl-3-(benzyloxy)-4(1*H*)-pyridinone (17) (70%): mp 169–170 °C. Anal. ($C_{17}H_{19}NO_4$) C, H, N.

1-(2′-Carboxyethyl)-2-methyl-3-hydroxy-4(1*H*)-pyridinone Hydrochloride (35). A solution of 16 (10 g, 0.035 mol) in ethanol (100 mL)/water (100 mL) was adjusted to pH 1 with hydrochloric acid prior to hydrogenolysis for 4 h in the presence of 5% Pd/C catalyst (0.5 g). Filtration followed by rotary evaporation gave a cream solid, recrystallization from ethanol/diethyl ether yielding a white powder (7.6 g, 93%): mp 207–208 °C. Anal. ($C_9H_{12}ClNO_4$) C, H, N.

An analogous procedure using 17 gave 1-(3′-carboxypropyl)-2-methyl-3-hydroxy-4(1*H*)-pyridinone (36) (90%): mp 225–226 °C. Anal. ($C_{10}H_{14}ClNO_4$) C, H, N.

1-[2′-[(Succinimidyloxy)carbonyl]ethyl]-2-methyl-3-(benzyloxy)-4(1*H*)-pyridinone (18). To a solution of 16 (10 g, 0.035 mol) in DMF (200 mL) was added *N*-hydroxysuccinimide (4 g, 0.035 mol) dissolved in DMF (50 mL) followed by *N*,*N*′-dicyclohexylcarbodiimide (7.2 g, 0.035 mol) dissolved in DMF (50 mL). After being stirred at room temperature for 18 h the resultant mixture was filtered and rotary evaporated to yield a white solid, recrystallization from dichloromethane/diethyl ether yielding a white powder (9.8 g, 73%): mp 144–146 °C. Anal. ($C_{20}H_{20}N_2O_6$) C, H, N.

1-[2′-(*N*-Methylcarbamoyl)ethyl]-2-methyl-3-hydroxy-4(1*H*)-pyridinone Hydrochloride (37). To a solution of 18 (5 g, 0.013 mol) in dichloromethane (100 mL) was added 40% aqueous methylamine (1 g, 0.013 mol) and the mixture stirred at room temperature for 4 h. After the solution was washed with water (3 × 100 mL) the organic layer was dried over anhydrous sodium sulfate, filtered, and rotary evaporated to give a yellow oil. This oil was subsequently dissolved in ethanol (90 mL)/water (10 mL) and adjusted to pH 1 with hydrochloric acid prior to room temperature hydrogenolysis for 4 h in the presence of 5% Pd/C catalyst (0.2 g). Filtration followed by rotary evaporation gave a white solid, recrystallization from ethanol/diethyl ether yielding a white powder (2.1 g, 62%): mp 182–183 °C. Anal. ($C_{10}H_{15}ClN_2O_3$) C, H, N.

Analogous procedures using a range of primary and secondary amines gave compounds 38 to 44 in Table X.

1-Decyl-2-methyl-3-hydroxy-4-(1*H*)-pyridinone Hydrochloride (28). To a solution of 5 (25 g, 0.12 mol) in ethanol (200 mL)/water (200 mL) was added decylamine (29 g, 0.18 mol) followed by 2 N sodium hydroxide solution (10 mL) and the mixture refluxed for 18 h. After adjustment to pH 1 with hydrochloric acid solvent was removed by rotary evaporation to give a red oil, which was reconstituted in ethanol (360 mL)/water (40 mL) and subjected to hydrogenolysis for 4 h in the presence of 5% Pd/C catalyst (1 g). Filtration followed by rotary evaporation gave an orange oil which was dissolved in water (500 mL) and washed with diethyl ether (2 × 500 mL) prior to adjustment to pH 7 with 10 N sodium hydroxide solution and extraction into dichloromethane (3 × 500 mL). The organic fractions were dried over anhydrous sodium sulfate, filtered, and rotary evaporated to give a yellow oil, which was reconstituted in ethanol/hydrochloric acid and rotary evaporated to yield a white solid. Recrystallization from ethanol/diethyl ether gave a white powder (20 g, 57%): mp 140–141 °C. Anal. ($C_{19}H_{28}ClNO_2$) C, H, N.

1-(2′-Aminoethyl)-2-methyl-3-hydroxy-4(1*H*)-pyridi-

Table X. Synthesis of 1-[2-(*N*-alkylcarbamoyl)ethyl]-2-methyl-3-hydroxy-4(1*H*)-pyridinone Hydrochlorides and Their Distribution Coefficients between an Aqueous Phase Buffered at pH 7.4 and Octanol

compd	R	R^1	mp, °C	% yield	formula	anal.	distribn coeff
37	Me	$(CH_2)_2CONHMe$	181–182	62	$C_{10}H_{16}N_2O_3Cl\cdot H_2O$	C,H,N	0.079 ± 0.003 (n = 5)
38	Me	$(CH_2)_2CONHEt$	156–157	63	$C_{11}H_{17}N_2O_3Cl\cdot H_2O$	C,[a]H,N	0.152 ± 0.003 (n = 5)
39	Me	$(CH_2)_2CONHPr$	156–157	77	$C_{12}H_{18}N_2O_3Cl\cdot{}^1/_2H_2O$	C,H,N	0.402 ± 0.003 (n = 6)
40	Me	$(CH_2)_2CONH^iPr$	103–104	70	$C_{12}H_{18}N_2O_3Cl\cdot1{}^1/_2H_2O$	C,H,N	0.338 ± 0.004 (n = 5)
41	Me	$(CH_2)_2CONHBu$	77–78	79	$C_{13}H_{21}N_2O_3Cl\cdot2H_2O$	C,[b]H,N	1.25 ± 0.06 (n = 7)
42	Me	$(CH_2)_2CON(Me)_2$	167–168	82	$C_{11}H_{17}N_2O_3Cl\cdot2{}^1/_2H_2O$	C,H,N	0.069 ± 0.001 (n = 5)
43	Me	$(CH_2)_2CONMeEt$	171–172	80	$C_{12}H_{19}N_2O_3Cl$	C,H,N	0.206 ± 0.001 (n = 5)
44	Me	$(CH_2)_2CON(Et)_2$	140–141	86	$C_{16}H_{21}N_2O_3Cl$	C,[c]H,N	0.436 ± 0.002 (n = 5)

[a] C: calcd, 47.39; found 46.91. [b] C: calcd, 48.06; found 48.56. [c] C: calcd, 54.06; found 53.61.

none Dihydrochloride (45). To a solution of **5** (25 g, 0.12 mol) in ethanol (200 mL)/water (200 mL) was added ethylenediamine (7 g, 0.12 mol) followed by 2 N sodium hydroxide solution (10 mL) and the mixture refluxed for 18 h. After adjustment to pH 1 with hydrochloric acid, volume was reduced to 200 mL by rotary evaporation prior to addition of water (200 mL) and washing with diethyl ether (400 mL). Subsequent adjustment of the aqueous fraction to pH 12 with 10 N sodium hydroxide solution was followed by extraction into dichloromethane (3 × 400 mL), the organic layers then being dried over anhydrous sodium sulfate, filtered, and rotary evaporated to give an orange oil. This oil was reconstituted in ethanol (150 mL)/water (150 mL) and adjusted to pH 1 with hydrochloric acid prior to hydrogenolysis for 4 h in the presence of 5% Pd/C catalyst (1 g). Filtration followed by rotary evaporation gave a white solid, recrystallization from ethanol yielding a white powder (17 g, 61%): mp 284–285 °C. Anal. ($C_9H_{14}Cl_2N_2O_2$) C, H, N.

An analogous procedure using 1,3-diaminopropane gave 1-(3′-aminopropyl)-2-methyl-3-hydroxy-4-(1*H*)-pyridinone dihydrochloride (**46**) (68%): mp 260–261 °C. Anal. ($C_9H_{16}Cl_2NO_2\cdot H_2O$) C, H, N.

Simultaneous Potentiometric and Spectrophotometric Titrations. Absorbance and emf were measured after incremental titrant addition using an automated system. This comprises a Corning Delta 250 pH meter, a Perkin-Elmer Lambda 5 UV/vis spectrophotometer and an autoburette interfaced to a PC microcomputer.

Parameters describing the model for iron(III) coordination by the hydroxypyridinone were optimized by nonlinear regression to minimize the sum of squared residuals between the simulated and true data using the program NONLIGEN15 (21) (in Microsoft Quickbasic 4.0). The stability constants were optimized from the spectrophotometric titration of the metal–ligand system using the pK_a values, electrode slope, and electrode zero determined above. Ionic strength was maintained at 0.1 with potassium nitrate (BDH Aristar grade). All solutions were made up with 18 MΩ cm^{-1} water from a Millipore Milli-Q system. Temperature was maintained at 22.5 ± 0.1 °C. Metal ion solutions were prepared from Fisons Analar nitrate salts and standardized by EDTA titration according to established procedures.[44] Absorbance was monitored at a wavelength of 305 nm at which the uncomplexed ligand has a low absorbance compared with the complex.

Determination of Distribution Coefficients. Partition coefficients were determined using an automated system based on a modified filter probe device.[20] The system comprised an IBM compatible PC running the "TOPCAT" program,[45] which controlled both a Metrohm 665 Dosimat autoburette and a Pye-Unicam Lambda 5 UV/vis spectrophotometer, as well as performing all calculations of partition coefficients. All partition coefficient determinations were performed using AnalaR grade reagents under a nitrogen atmosphere in a sealed titration vessel at 25 °C. To ensure effective partition of the sample compound, continuous rapid stirring was employed, such that an emulsion of the two immiscible phases was formed. Use of a hydrophilic (Schleicher and Schueu 589/3) blauband filter paper on the filter probe ensured that none of the hydrophobic phase was measured, even with the small droplet sizes generated by the stirring. The ability to vary the volume of the two phases over a wide range (aqueous phase, 10–190 mL; nonaqueous phase, 0.1 μL–190 mL) enabled determination of partition coefficients in the range 10^{-5}–10^5 to be determined, as evidenced by measurement of partition coefficients of a series of test compounds.[46] The two phases used in the determinations were MOPS buffer (50 mM, pH 7.4, prepared using Milli-Q water) and octan-1-ol, each of which was preequilibrated with the other phase before use. The solutions were gently purged with nitrogen. Upon commencement of the determination, absorbance measurements were automatically recorded at preselected time intervals, usually 1 s. When the absorbance readings had stabilized, as determined by the computer from equilibrium conditions selected by the operator (typically defined as an absorbance change of less than 0.002 absorbance units over a minimum of 100 individual readings), a suitable volume of octan-1-ol was added from the autoburette. Absorbance readings were subsequently recorded until the system had again reached equilibrium, at which point a further aliquot of octan-1-ol was added. This cycle was repeated for at least 10 additions of octan-1-ol. An estimate of the partition coefficient was obtained from each octan-1-ol addition, which enabled calculation of a mean partition coefficient value and standard deviation.

Table XI. Experimental Data and Final Refinement Results for **49**, **49·HCl**, and **58**

	49	**49·HCl**	**58**
formula	$C_9H_{13}NO_2$	$C_9H_{13}NO_2\cdot HCl\cdot H_2O$	$C_{27}H_{36}FeN_3O_9\cdot 3H_2O$
formula wt	167.36	221.69	656.50
space group	$P2_1/n$	$P2_1/a$	$P\bar{3}$
a/Å	7.1025(6)	7.8933(7)	15.406(5)
b/Å	9.3441(9)	18.073(1)	
c/Å	13.495(1)	7.8424(4)	7.214(3)
β°	92.682(8)	98.588(4)	120.00
V/Å^3	894.7(4)	1106.2(7)	1482.6(9)
Z	4	4	2
D_c/g cm^3	1.25	1.34	1.48
radiatn	Cu K$\bar{\alpha}$	Cu K$\bar{\alpha}$	Mo K$\bar{\alpha}$
wavelength Å	1.541 78	1.541 78	0.710 73
T K	132(2)	132(2)	132(2)
$2\sigma max/\lambda$ = deg	150	150	53
total data	2119	2533	2029
obsd data	1480 ($I \geq 2(I)$)	1823 ($I \geq 2(I)$)	1332 ($I \geq 5(I)$)
R	0.046	0.039	0.068

X-ray Experimental. Compounds **49** and **49·Cl**, and **58** were crystallized from ethanol/hexane, acetonitrile/cyclohexane, and dimethylformamide/heptane diffusion systems, respectively, at 4 °C. All data were taken on an Enraf-Nonius CAD4 diffractometer, using a $\omega - 2\omega$ scan technique. Lorentz-polarization corrections were applied. No absorption correction was made. Structures **49** and **49·HCl** were solved by direct methods using SHELX86[47] and refined by full-matrix least-squares minimization of $\sum w (F_o - KF_c)^2$), where $w = 1/\sigma^2(F_o)$ using SHELX76.[48] In structure **58** the Fe atom was located on a special position on the 3-fold axis in space group $P\bar{3}$. The structure was refined with appropriate thermal parameter restraints for the Fe atom, using $w = 1/(\sigma^2(F_o) + 0.0005F_o^2)$. The terminal methyl group C(10) was found to be dynamically disordered even at 132 K. Three peaks were located bonded to the O(9) atom on the difference Fourier map and fixed through the refinement. The experimental data and final refinement results for **49**, **49·HCl**, and **58** are presented in Table XI. Full crystallographic details are available as supplementary material.

Biological Methods: Iron Removal from Proteins. Transferrin. Human transferrin (Sigma) was dissolved in MOPS

buffer (0.05 M, pH 7.4, 25 °C) containing 25 mM $NaHCO_3$. Transferrin concentration was determined using an extinction coefficient of 2310 M^{-1} cm^{-1} per iron atom on the basis of a protein molecular mass of 81 000.[49] Solutions were monitored spectrophotometrically between 400–500 nm at 2-min intervals for the initial 10-min period and subsequently at 5-min intervals for periods up to 3 h.

Ferritin. Horse spleen ferritin (Boehringer) was incubated in HEPES (0.1 M, pH 7.2, 37 °C) with a range of chelators. One-mL samples were removed at given time intervals and immediately centrifuged through Amicon Centriflo ultrafiltration membrane cones to separate the hydroxypyridinone–Fe(III) complex from ferritin. The concentrations of Fe(III) complex were determined from ϵ_{max} values. Time courses of iron release was investigated for periods up to 36 h.

Iron Removal from Rat Hepatocytes. Primary rat hepatocyte monolayers were isolated, cultured, and pulsed with ^{59}Fe–transferrin.[16] Briefly, cells were plated at 1×10^6/dish and left for 4 h to adhere. Following washing, hepatocytes were pulsed for 17 h with human diferric ^{59}Fe–transferrin (100 μg/mL) before washing excess transferrin free with fresh medium. Cells were then incubated in triplicate with chelators at the concentrations shown, medium removed at 6 h, and the cells washed three times before being scraped from the plate with a rubber policeman and suspended in phosphate buffered saline. ^{59}Fe was measured in supernatant and expressed as a fraction of total cellular ^{59}Fe at time zero. Results are expressed as a percentage of ^{59}Fe release in control cells (medium without chelators added). Aliquots of supernatant were taken for measurement of LDH[16] and aliquots of cells for measurement of malonyl dialdehyde (MDA) and cellular DNA.[16] The MDA assay was adapted from previously described procedures using the thiobarbituric acid (TBA) assay method.[50] Standard curves were constructed using tetramethoxypropane (100–700 nM). One mL of standard or homogenized cells in phosphate-buffered saline were added to 1 mL of TBA solution (0.8%, pH 7.4) and incubated at 90 °C for 30 min. Cells were immediately cooled on ice and spun at 3000 rpm at 4 °C for 10 min. The red color was measured spectrophotometrically at 532 nm, corrected for cellular DNA content, and expressed as a percentage of the MDA present in control cells.

Iron Removal from Iron-Overloaded Mice. A modification of the mouse model developed by Huehns and co-workers was used.[51] The mice were overloaded with iron dextran given intraperitoneally at weekly intervals for 4 weeks. The iron stores were then radiolabeled with [^{59}Fe]lactoferrin. This treatment preferentially delivers iron to the liver.[52] Iron excretion was allowed to equilibrate for 3 weeks when a plateau was reached. At this stage the mice were used to measure the ^{59}Fe excretion induced by the test compounds given intraperitoneally. Both feces and urine were collected separately over defined time periods for a number of days, and the ^{59}Fe excretion was monitored. The excretion following the administration of each compound was expressed as a percentage of the counts excreted during the previous 24-h period.

Acknowledgment. This research was supported by the British Technology Group and NIH (Project Grants: GK42800 and GM21822).

Supplementary Material Available: Full elemental and spectral analyses of compounds **5–56** and tables of X-ray final atomic positional coordinates, atomic thermal parameters, bond distances, and bond angles of **49**, **49**·HCl, and **58** (19 pages). Ordering information is given on any current masthead page.

References

(1) Weatherall, D. J.; Clegg, J. B. *The Thalassaemia Syndromes*, 3rd ed.; Blackwell Scientific Publications: Oxford, 1981.
(2) Halliwell, B.; Gutteridge, J. M. C. Oxygen toxicity, oxygen radicals, transition metals and disease. *Biochem. J.* **1984**, *219*, 1–4.
(3) Sephton-Smith, R. Iron excretion in thalassaemia major after administration of chelating agents. *Brit. Med. J.* **1962**, *2*, 1577–1580.
(4) Modell, B.; Letsky, E. A.; Flynn, D. M.; Peto, R.; Weatherall, D. J. Survival and desferrioxamine in thalassaemia major. *Brit. Med. J.* **1982**, *284*, 1081–1084.
(5) Porter, J. B.; Huehns, E. R.; Hider, R. C. The development of iron chelating drugs. In *Ballière's Clinical Haematology*; Hershko, C., Ed.; Bailliése Tindall: London, 1989; Vol. 2, pp 257–292.
(6) Rodgers, S. J.; Lee, Chi-Woo; Ng, C. Y.; Raymond, K. N. Ferric iron sequestering agents. 15. Synthesis, solution chemistry and electrochemistry of a new cationic analogue of enterobactin. *Inorg. Chem.* **1987**, *26*, 1622–1625.
(7) Bergeron, R. J.; Wiegand, J.; McManis, J. S.; Perumal, P. T. Synthesis and biological evaluation of hydroxamate-based iron chelators. *J. Med. Chem.* **1991**, *34*, 3182–3187.
(8) Martell, A. E.; Motekaitis, R. J.; Clarke, E. T.; Harrison, J. J. Synthesis of N,N′-di(2-hydroxybenzyl)ethylenediamine-N,N′-diacetic acid (HBED) derivatives. *Can. J. Chem.* **1986**, *64*, 449–456.
(9) Hider, R. C. Siderophore mediated absorption of iron. *Struct. Bond.* **1984**, *38*, 25–87.
(10) Hider, R. C.; Hall, A. D. Clinical useful chelators of tripositive elements. In *Progress in Medicinal Chemistry*; Ellis, G. P., West, G. B., eds.; Elsevier: New York, 1991; Vol. 28, pp 41–173.
(11) Summers, J. B.; Gunn, B. P.; Martin, J. G.; Mazdiyasni, H.; Stewart, A. O.; Young, P. R.; Goetze, A. M.; Bousko, J. B.; Dyer, R. D.; Brooks, D. W.; Carter, G. W. Orally active hydroxamic acid inhibitors of leukotriene biosynthesis. *J. Med. Chem.* **1988**, *31*, 3–5.
(12) Hershko, C.; Link, G.; Pinson, A.; Avramovia-Grisaru, S.; Sarel, S.; Peter, H. H.; Hider, R. C.; Grady, R. W. New orally active iron chelators. *Ann. N. Y. Acad. Sci.* **1990**, *612*, 351–360.
(13) (a) Hider, R. C.; Kontoghiorghes, G.; Silver, J.; Stockham, M. A. UK Patent 2117766, 1982. (b) Hider, R. C.; Kontoghiorghes, G.; Silver, J. UK Patent 2118176, 1983. (c) Hider, R. C.; Kontoghiorghes, G.; Silver, J. UK Patent 2136807, 1983. (d) Hider, R. C.; Kontoghiorghes, G.; Silver, J.; Stockham, M. A. UK Patent 2146989, 1984. (e) Hider, R. C.; Kontoghiorghes, G. K.; Silver, J.; Stockham, M. A. UK Patent 2146990, 1984. (f) Kontoghiorghes, G. K. Orally active α-ketohydroxypyridinone iron chelators: Studies in mice. *Mol. Pharmacol.* **1986**, *30*, 670–673.
(14) Scarrow, R. C.; Riley, P. E.; Abu-Dari, K.; White, D. L.; Raymond, K. N. Ferric iron sequestering agents. 13. Synthesis structures and thermodynamics of complexation of Co(III) and Fe(III) tris complexes of several chelating hydroxypyridinones. *Inorg. Chem.* **1985**, *24*, 952–967.
(15) Streater, M.; Taylor, P. D.; Hider, R. C.; Porter, J. B. Novel 3-hydroxy-2(1*H*)-pyridinones. Synthesis, iron(III)-chelating properties and biological activity. *J. Med. Chem.* **1990**, *33*, 1749–1755.
(16) Porter, J. B.; Gyparaki, M.; Burke, L. C.; Huehns, E. R.; Sarpong, P.; Saez, V.; Hider, R. C. Iron metabolisation from hepatocyte monolayer cultures by chelators: the importance of membrane permeability and the iron binding constant. *Blood* **1988**, *72*, 1497–1503.
(17) Hider, R. C.; Taylor, P. D.; Walkinshaw, M.; Wang, J. L.; van der Helm, D. Crystal structure of 3-hydroxy-1,2dimethylpyridin-4(1*H*)-one: An iron(III) chelation study. *J. Chem. Res., Synop.* **1990**, 316–317.
(18) (a) Harris, R. L. N. Potential wool growth inhibitors. Improved synthesis of mimosine and related 4(1*H*)-pyridinones. *Aust. J. Chem.* **1976**, *29*, 1329–1334. (b) Stünzi, H.; Perrin, D. D.; Teitei, T.; Harris, R. L. N. Stability constants of some metal complexes formed by mimosine and related compounds. *Aust. J. Chem.* **1979**, *32*, 21–30. (c) Stünzi, H.; Harris, R. L. N.; Perrin, D. D.; Teitei, T. Stability constants for metal complexation by isomers of mimosine and related compounds. *Aust. J. Chem.* **1980**, *33*, 2207–2220.
(19) Le Blanc, D. T.; Akers, H. A. Maltol and ethylmaltol. *Food Technol. (Chicago)* **1989**, *43*, 78–84.
(20) Tomlinson, E. Filter probe extractor: A tool for the rapid determination of oil–water partition coefficients. *J. Pharm. Sci.* **1982**, *71*, 602–604.
(21) Taylor, P. D.; Morrison, I. E. G.; Hider, R. C. Microcomputer application of non-linear regression analysis to metal-ligand equilibria. *Talanta* **1988**, *35*, 507–512.
(22) Nelson, W. O.; Rettig, S. J.; Orvig, C. Aluminum and gallium complexes of 1-ethyl-3-hydroxy-2-methyl-4-pyridinone: A new exoclathrate matrix. *Inorg. Chem.* **1989**, *28*, 3153–3157.
(23) Xiao, G.; van der Helm, D.; Hider, R. C.; Dobbin, P. S. Structure-stability relationships of 3-hydroxypyridin-4-one complexes. *J. Chem. Soc., Dalton Trans.* **1992**, 3265–3271.
(24) Nelson, W. O.; Karpishin, T. B.; Rettig, S. J.; Orvig, C. Physical and structural studies of N-substituted-3-hydroxy-4(1*H*)-pyridinones. *Can. J. Chem.* **1988**, *66*, 123–131.
(25) Xiao, G.; van der Helm, D.; Georlitz, F. H.; Hider, R. C.; Dobbin, P. S. The crystal structures of 1-(2′-methoxyethyl)-2-methyl-3-hydroxy-4-pyridinone, its hydrochloride and 1-ethyl-2-methyl-3-hydroxy-4-pyridinone hydrochloride hydrate. *Acta Crystallogr. C.*, in press.
(26) Nelson, W. O.; Karpishin, T. B.; Rettig, S. J.; Orvig, C. Aluminum and gallium compounds of 3-hydroxy-4-pyridinones. Synthesis characterisation and crystallography of biologically active complexes with unusual hydrogen bonding. *Inorg. Chem.* **1988**, *27*, 1045–1051.

(27) Charalambous, J.; Dodd, A.; McPartlin, M.; Matondo, S. O. C.; Pathirana, N. D.; Powell, H. R. Synthesis and x-ray crystal structure of tris(1,2-dimethyl-3-hydroxypyrid-4-onato)iron(III). *Polyhedron* 1988, *7*, 2235–2237.
(28) Simpson, L.; Rettig, S. J.; Trotter, J.; Orvig, C. 1-n-Propyl and 1-n-butyl-3-hydroxy-2-methyl-4-pyridinone complexes of group 13 (IIIA) metal ions. *Can. J. Chem.* 1991, *69*, 893–900.
(29) Brady, M. C.; Lilley, K. S.; Treffry, A.; Harrison, P. M.; Hider, R. C.; Taylor, P. D. Release of iron from ferritin molecules and their iron-cores by 3-hydroxypyridinone chelators *in vitro*. *J. Inorg. Biochem.* 1988, *35*, 9–22.
(30) Porter, J. B.; Gyparaki, M.; Huehns, E. R.; Hider, R. C. The relationship between lipophilicity of hydroxypyrid-4-one iron chelators and cellular iron metabolism using an hepatocyte culture model. *Biochem. Soc. Trans.* 1986, *14*, 1180.
(31) Porter, J. B.; Morgan, J.; Hoyes, K. P.; Burke, L. C.; Huehns, E. R.; Hider, R. C. Relative oral efficacy and acute toxicity of hydroxypyridin-4-one iron chelators in mice. *Blood* 1990, *76*, 2389–2396.
(32) Motekaitis, R. J.; Martell, A. E. Stabilities of the iron(III) chelators of 1,2-dimethyl-3-hydroxy-4-pyridinone and related ligands. *Inorg. Chim. Acta* 1991, *183*, 71–80.
(33) pM = log $[Fe^{3+}]$ in the presence of $[Fe^{3+}]_{total} = 10^{-6}$ M and $[ligand]_{total} = 10^{-5}$ M at pH 7.4.
(34) Smith, R. M.; Martell, A. E. *Critical Stability Constants*; Plenum: New York, 1989; Vols. 1–6.
(35) Gerard, G.; Hugel, R. P. Iron(III) complexes of maltol including hydroxo-complexes, in an acidic medium. *J. Chem. Res., Synop.* 1980, 314.
(36) Bullen J. J.; Griffiths, E. *Iron and Infection*; Wiley: London, 1987.
(37) Stefanini, S.; Chiancone, E.; Cavallo, S.; Saez, V.; Hall, A. D.; Hider, R. C. The interaction of hydroxypyridinones with human serum transferrin and ovotransferrin. *J. Inorg. Biochem.* 1991, *44*, 27–37.
(38) Ford, G. C.; Harrison, P. M.; Rice, D. W.; Smith, J. M. A.; Treffry, A.; White, J. L.; Yariv, J. Ferritin: Design and formation of an iron-storage molecule. *Phil. Trans. Royal Soc. London B* 1984, *304*, 551–565.
(39) Gyparaki, M.; Hider, R. C.; Huehns, E. R.; Porter, J. B. Hydroxypyridinone iron chelators: *in vitro* and *in vivo* evaluation. *Thalassaemia Today* (Sirchia, G., Zanella, A., Eds.) Centro Transfusionale Ospedale Maggoire Polioclinico di Milano Editore, 1987, 521–526.
(40) Porter, J. B.; Morgan, J.; Hoyes, K. P.; Burke, L. C.; Huehns, E. R.; Hider, R. C. Relative oral efficacy and acute toxicity of hydroxypyridin-4-one iron chelators in mice. *Blood* 1990, *76*, 2389–2396.
(41) Porter, J. B.; Weir, T. B.; Marshall, L.; Abeysinghe, R.; Round, J. M.; Brenton, D.; Huehns, E. R.; Epemolu, R. O.; Singh, S.; Dobbin, P. S.; Hider, R. C. Dose escalation and iron balance studies with the orally active hydroxypyridin-4-one iron chelator, CP94 in transfusionally iron overloaded humans. *Blood*, in press.
(42) Tondury, P.; Kontoghiorghes, G. J.; Ridolfi-Luthy, A.; Hirt, A.; Hoffbrand, A. V.; Lottenbach, A. M.; Sonderegger, T.; Wagner, H. P. L1 (1,2-dimethyl-3-hydroxypyrid-4-one) for oral iron chelation in patients with β-thalassaemia major. *Brit. J. Haematol.* 1990, *76*, 550–553.
(43) Brittenham, G. M. Development of iron-chelating agents for clinical use. *Blood* 1992, *80*, 569–575.
(44) Harris, W. R.; Carrano, C. J.; Cooper, S. R.; Sofen, S. R.; Avdeef, A. E.; McArdle, J. V.; Raymond, K. N. Co-coordination chemistry of microbial iron transport compounds. 19. Stability constants and electrochemical behaviour of ferric enterobactin and model complexes. *J. Am. Chem. Soc.* 1979, *101*, 6097–6104.
(45) Hall, A. D. TOPCAT Program for Determination of Distribution Coefficients, King's College, University of London, 1990.
(46) Sarpong, P. Ph.D. Thesis, University of London, 1992.
(47) Sheldrick, G. M. SHELX86. Programe for the Solution of Crystal Structures, University of Gottingen, Germany, 1986.
(48) Sheldrick, G. M. SHELX76. Program for the Solution of Crystal Structures, University of Cambridge, England, 1976.
(49) Aisen, P. In *Transferrin in Iron in Biochemistry and Medicine*; Jacobs, A., Worwood, M., Eds.; Academic Press: London, 1980; Vol. 2, 87–102.
(50) Stuart, M. J.; Scott, M.; Oski, F. A. A simple non-radioisotope technique for the determination of platelet life-span. *New Eng. J. Med.* 1975, *19*, 1310–1316.
(51) Gyparaki, M.; Porter, J. B.; Hirani, S.; Streater, M.; Hider, R. C.; Huehns, E. R. *In vivo* evaluation of hydroxypyridinone iron chelators in a mouse model. *Acta Haematol.* 1987, *78*, 217–221.
(52) Van Snick, J.; Mason, P. L.; Hermans, J. F. In *Proteins of Iron Storage and Transport in Biochemistry and Medicine*; North-Holland/Elsevier: Amsterdam, 1975; pp 433–438.